Science and Technology Indonesia
e-ISSN:2580-4391 *p*-ISSN:2580-4405
Vol. 9, No. 2, April 2024

Research Paper

Synthesis of Ion Imprinted Polymers (IIPs) Adsorbent Materials Using Fe(III) Leaching Process with Variation of Hydrochloric Acid Solvent Concentration and Heat Treatment

Idha Royani[1,2,3]*, Maimunah[2], Jaya Edianta[2], Ihsan Alfikro[1,2], Fiber Monado[1,2], Jorena[1], Octavianus Cakra Satya[1], Frinsyah Virgo[1]

[1]*Department of Physics, Faculty of Mathematics and Natural Sciences, Universitas Sriwijaya, Indralaya, 30662, Indonesia*
[2]*Laboratory of Material Science, Department of Physics, Faculty Mathematic and Natural Science, Universitas Sriwijaya, Indralaya, 30662, Indonesia*
[3]*Master Program of Material Science, Graduate School, Universitas Sriwijaya, Palembang, 30139, Indonesia*
***Corresponding author**: idharoyani@unsri.ac.id

Abstract
Fe(III)-IIPs material was prepared using a cooling-heating method with different leaching variations. The synthesis process used several chemical components, including EGDMA, MAA, and BPO as the crosslinker, functional monomer, and initiator. This study focused on the template formation process of IIPs with leaching variations, using parameters such as molarity concentration, solution mixture, and temperature to influence the amount of template formed in the polymer body. The spectra of XRD showed a widening value of FWHM as higher molarity was applied during the leaching process, with the widest one at 0.163 rad for IIPs 3 M. Fe(III) peak is located at 680-610 cm^{-1} or 1386-1350 cm^{-1} within the unleached sample, according to FTIR spectra. It also can be traced at minimum intensity in leached samples. SEM data processing showed that higher concentrations were essential in releasing Fe(III) ions from the polymer body. Meanwhile, heat treatment did not strongly impact the template formation sites of IIPs. Synthesized Fe(III)-IIPs materials had adsorption capacity, optimum time, and efficiency of 9.35 $mg.g^{-1}$, 40 minutes, and 93.48%, respectively. Based on the results, Fe(III)-IIPs materials had great potential as adsorbents for removing metal pollutants from water.

Keywords
Ion Imprinted, Fe(III), Leaching, Cooling-Heating, Adsorption

Received: 16 November 2023, Accepted: 21 February 2024
https://doi.org/10.26554/sti.2024.9.2.336-344

1. INTRODUCTION

The rapid development of modern industries, including pesticide fabrication and metals in the era of Industry 4.0, has led to a significant increase in the presence of heavy metal waste in the environment (Abbas et al., 2016). In addition, the quantification of heavy metal ions levels poses various challenges, impacting both the environment and human health. Among the hazardous heavy metals prevalent in chemical and hydrometallurgical industries, iron (Fe^{3+}) stands out due to its coexistence, capable of degrading the quality of industrial products (Zhu et al., 2020). The presence of Fe^{3+} metal ions has been reported to exacerbate the quality of drinking water due to the tendency to deposit sludge in air-exposed pipelines, thereby altering the taste, odor, and color of the water. According to the World Health Organization (WHO), the maximum allowable concentration of Fe^{3+} in drinking water is 0.3 $mg.L^{-1}$ (Mahmoud, 2015). To overcome this problem, several studies successfully developed conventional synthesis methods for various materials with remarkable abilities to the ions from aquatic sites. These methods include membrane technology (Kasim et al., 2016), chemical precipitation (Izadi et al., 2017), ion-exchange (Bezzina et al., 2020), coagulation (Wyns et al., 2021), and carbon adsorption using nanotechnology (Edianta et al., 2023b).

Several studies showed that adsorption methods offered superior advantages compared to other conventional methods due to their efficiency, flexibility, and high regeneration capability. With these characteristics, adsorbent materials emerge as fundamental remediation tools with excellent selectivity and capacity, particularly when dealing with a complex sample matrix (Adibmehr and Faghihian, 2019). Among the physical adsorption materials, Ion Imprinted Polymers (IIPs) have proven to be effective in removing various heavy metal ions from the environment. IIPs are advanced materials with significant advantages, including excellent selectivity and sensitivity. In addition, IIPs find applications as both adsorbents and electrochemical sensors, making them functional components with high selectivity, relatively low cost, and efficient processing time (Sala et al., 2022). This has led to the widespread development of these materials by several studies to eliminate or adsorb various heavy metals in water, such as Al(III), Be(II), Ce(IV),

Ni(II), As(III), Ru(III), Cr(VI), Cd(II), Cu(II), Co(II), Hg(II), Pb(II) (Ahmadi et al., 2021; Cao et al., 2021; Chi et al., 2021; Kong et al., 2021; Mhatre et al., 2021; Rais et al., 2021; Taheri et al., 2021; Wang et al., 2022; Zhang et al., 2021; Zhao et al., 2022) including Fe(III) metal ions (Mitreva et al., 2017).

IIP has been widely used as a metal adsorbent material with selective properties towards the targeted metal by attaching to the printed polymer sites; various methods employed using a solid absorbent for the extraction of ions in solution such as ion exchange precipitation (Reis et al., 2024) and co-precipitation solvent extraction chemical (Huang et al., 2024) and biosorption could point extraction (Diale et al., 2023), solid phase-extraction (Rivaro et al., 2024) and on-line flow injection (Ricart et al., 2024). Several studies on the development of Fe(III)-IIPs have utilized dry nitrogen (Darmawan et al., 2020; Mitreva et al., 2017; Roushani et al., 2016) to suck up potential reactive gas from pre-polymerization solution. This study aims to discuss the synthesis process of IIPs materials for removing Fe(III) metal ions using the cooling-heating method. The latest cooling heating method has been widely researched to form active polymers that can recognize several dangerous molecules in water, such as atrazine (Royani et al., 2014), melamine (Koriyanti et al., 2020), and caffeine (Royani et al., 2021). Edianta et al. (2023a) conducted research in measuring the concentration of Fe^{3+} ions by optimizing polymer imprinted ions and utilizing Arduino Uno-based instrumentation. Novianty et al. (2023) have also conducted research on ion-imprinted polymers by optimizing the effect of acid solution concentration on the Fe(III) ion extraction process to determine the number of cavities formed in Fe(III)-IIPs. The cooling-heating process utilizes temperature in the polymerization process by optimizing time, which is more effective and cost-effective. The synthesis process was optimized and characterized by speed fast, adjustability, and safety.

The synthesis process was optimized and characterized by speed fast, adjustability, and safety. This study focuses on the process of removing the active substance, serving as the template for IIPs, with various leaching variations. The parameters used during the procedure included molarity concentration, solution mixture, and the influence of extraction temperature on the amount of template formed in the polymer body. To determine the physical properties and characteristics of the material, IIPs were fully characterized using XRD to determine the structure arrangement and crystal size. In addition, FTIR was carried out to analyze the functional groups, chemical bonds, and polymer transmittance percentage, while SEM was used to determine the morphology and wide surface imaging of the polymer. The experimental analysis of IIPs adsorption on Fe^{3+} metal ions was performed through physisorption and tested using AAS equipment to determine the remaining concentration of Fe^{3+} metal ions after the adsorption process.

2. EXPERIMENTAL SECTION

2.1 Materials

The materials required in the synthesis process were iron(III) nitrate nonahydrate ($Fe(NO_3)_3.9H_2O$) as the active substance forming the template, methacrylic acid ($C_4H_6O_2$) as the functional monomer, benzoyl peroxide ($C_{14}H_{10}O_4$) as a free radical initiator, ethylene glycoldimethacrylate ($C_{10}H_{14}O_4$) as a crosslinker, and various solvents, such as ethanol (C_2H_6O) as a porogen solvent, distilled water, and deionized water as a pure solvent and template cleansers, as well as hydrochloric acid (HCl) as a solvent in leaching process. All materials used were from Merck Germany.

2.2 Instrument

The characterization tools used to determine the material properties included the X-Ray Diffractometer (XRD) (Rigaku Miniflex 600 series) for identifying the crystal system arrangement of IIPs samples, Fourier Transform Infrared (FTIR) Spectrometer (Nicolet iS10 series) for analyzing functional groups, chemical bonds, and sample transmittance percentage, Scanning Electron Microscope (SEM) (Tescan Vega III) for analyzing the surface morphology of the samples, and Atomic Absorption Spectroscopy (AAS) (Shimadzu AA-7000 series) for analyzing the results of Fe^{3+} metal ions adsorption experiment

2.3 Synthesis Process of Fe(III)-IIPs Using the Cooling-Heating Method

Fe(III)-IIPs pre-polymer solution was prepared by dissolving the template-forming active substance $Fe(NO_3)_3.9H_2O$, 0.404 g, in 40 mL ethanol solvent. Subsequently, methacrylic acid (0.4 mL), ethylene glycoldimethacrylate (3.9 mL), and benzoyl peroxide (0.07 g) were added sequentially to the beaker. Pre-polymer solution was then homogenized using a hot plate and magnetic stirrer for 90 minutes at a constant temperature of 25 °C. The solution was transferred into a vial and tightly sealed for the cooling process in a refrigerator at -5 °C for 1 hour. The heating process was carried out using a furnace at 60 °C for 24 hours. The resulting solid polymer was then ground and characterized using FTIR, XRD, SEM, and AAS. Non-ion imprinted Polymer (NIP) was synthesized using the same stages and procedures without the use of Fe(III) active substance.

2.4 Leaching Process of IIPs on Fe(III) Metal Ion

Fe(III) polymer powder obtained was subjected to a washing process: (1) A total of 0.3 gr Fe(III) polymer sample was soaked in 3 mL ethanol for 4 hours, filtered, and soaked again in ethanol, with 15 repetitions. (2) Polymer powder obtained from stage 1 was soaked using deionized water and 1.5 mL ethanol (1:20) repeatedly for 4 hours, with a total of 15 repetitions. (3) Polymer powder obtained from stage 2 was extracted with several acid solvent (HCl) parameters such as concentration/molarity, as well as the effect of temperature on template

© 2024 The Authors.

Table 1. Variations in the Leaching Process for the Formation of Fe(III)-IIPs Templates

Sample	Leaching Process Parameters				
	Solvent	Volume (mL)	Concentration (M)	Temp. (°C)	Time (hour)	Recurrence (times)
IIPs 3 M	HCl	3	3	room	12	5
IIPs 1 M	HCl	3	1	room	12	5
IIPs hot 1 M	HCl	3	1	60	12	5
IIPs hot 1,5 M	HCl	3	1.5	60	12	5

Table 2. Distribution of Fe(III) Crystal Sizes Calculated Using the Debye Schererr Equation

Sample	Temperature of Heating	2θ (°)	FWHM (rad)	Crystal Size D (nm)
Ferryc Nitrate	Room T	22.1	0.01395	10.120
Poymer Fe(III) unleached	Room T	16.33	0.163105	0.857
IIPs 3 M	Room T	15.6	0.16746	0.835
IIPs 1 M	Room T	16.4	0.15874	0.880
IIPs hot 1 M	60 °C	16.4	0.15002	0.931
IIPs hot 1.5 M	60 °C	16.5	0.15229	0.919

formation in Fe(III)-IIPs, as shown in Table 1. (4) Each sample was given the same treatment, namely soaking in 3 mL deionized water every 4 hours for 4 repetitions to neutralize IIPs sample to pH 7.

The samples were then dried in a heating oven at a temperature of 50°C for 1 hour. Subsequently, all 4 samples were characterized using XRD, FTIR, SEM, and EDX.

2.5 Adsorption Experiment

Fe(III) metal ions adsorption experiments were carried out using IIPs as experimental objects. Adsorption capacity (q_t) and absorption efficiency (%re) of IIPs materials towards Fe(III) metal ions were analyzed using Equation (1) and Equation (2).

$$q_t = \frac{C_i - C_t}{m} \times V \quad (1)$$

$$\%re = \frac{C_i - C_t}{C_i} \times 100\% \quad (2)$$

C_i and C_t are quantities that express the concentration of the target metal ion, namely Fe(III), before and after undergoing adsorption process using IIPs in ppm units. The instrument used to confirm the presence of Fe(III) metal ions in solution was the Atomic Absorption Spectroscopy (AAS). In this stage, 10 mg Fe(III)-IIPs materials were added to the 10 ppm Fe(III) solution, stirred for several minutes, and left for varying adsorption times of 20, 30, 40, and 50 minutes. In addition, adsorption data was modeled into pseudo-first-order (PFO) (3) and pseudo-second-order (PSO) (4) Equations.

$$q_t = q_e(1 - e^{-k_1 t}) \quad (3)$$

$$q_t = \frac{q_e^2 k_2 t}{1 + q_e k_2 t} \quad (4)$$

The parameters used to assess the suitability of data with non-linear modeling included AIC (Akaike Information Criterion), BIC (Bayesian Information Criterion), and SE (standard error estimate), which were calculated using Rstudio statistical software.

3. RESULTS AND DISCUSSION

3.1 Analysis of Fe(III)-IIPs Materials Synthesis Process Using the Cooling-Heating Method

Fe(III)-IIPs materials were successfully synthesized using several chemical components, such as Iron(III) nitrate nonahydrate, EGDMA, MAA, and BPO as the template-forming analyte, cross-linking polymer binder, functional monomer, and initiator, respectively. The synthesis process of the material is presented in Figure 1. Fe(III)-IIPs materials were processed using the cooling-heating method. In the cooling process, cold temperature was used to eliminate the oxygen content in the pre-polymer solution, which served as an inhibitor for the interaction between Fe(III) metal analyte and functional monomer during free radical polymerization. Subsequently, the heating process caused the evaporation of ethanol in pre-polymer solution. During the heating process, high temperature led to an increase in the viscosity of pre-polymer solution over time. After 24 hours, a stage change from pre-polymer solution to the solidification stage occurred, leading to the transformation of polymer solution into a perfect acrylic solid. This acrylic solid was then ground to produce a powder, which was referred to as Fe(III) polymer.

3.2 Analysis of Leaching Process in the Formation of Fe(III)-IIPs Templates

Fe(III) polymer was subjected to a washing stage using deionized water and ethanol before leaching. The use of ethanol as a washing solution was carried out to remove any remaining

© 2024 The Authors.

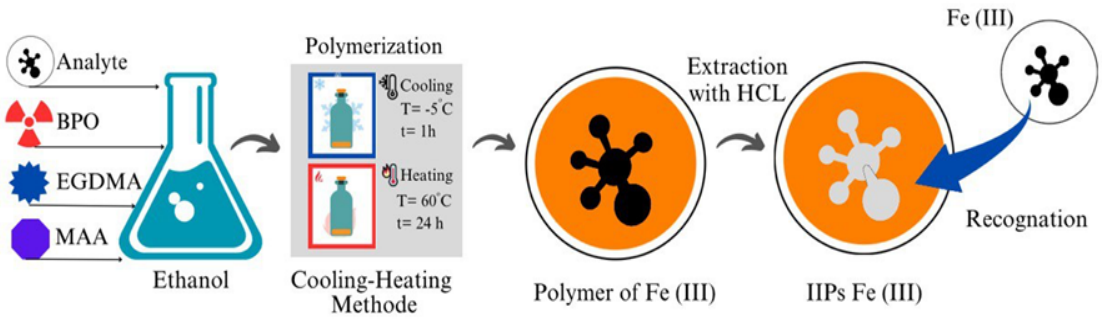

Figure 1. llustration of the Synthesis and Sample Preparation of IIPs Using the Cooling-Heating Method with Leaching Optimization Using HCl for Fe(III) Removal.

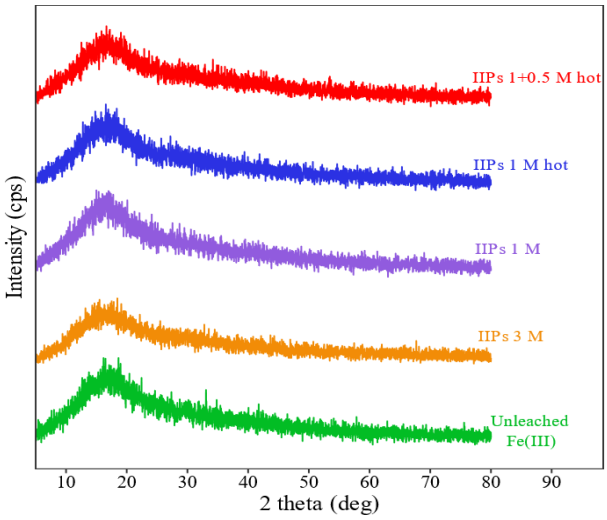

Figure 2. Sample Characterization Results: without Extraction Process (black), 3 M Fe(III)-IIPs (red), 1 M Fe(III)-IIPs (blue), 1 M IIPs with Heating (green), and 1.5 M IIPs with Heating (pink color)

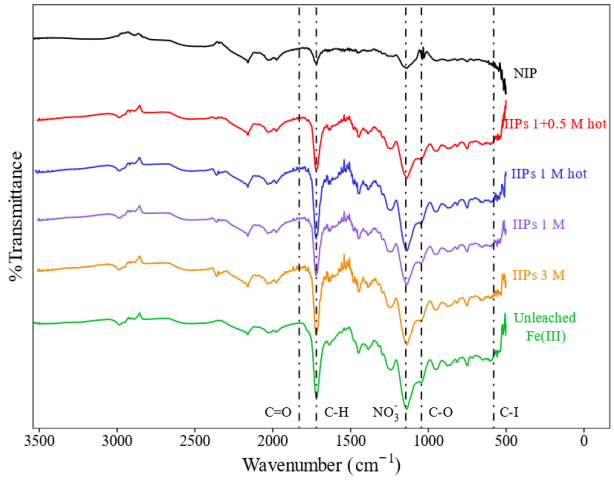

Figure 3. Results of FTIR Characterization of Unleached IIPs and Leached IIPs Materials Using HCl Solution

chemical components that did not react with each other, such as bonds between active substances and functional monomers or cross-linking occurring during the cooling-heating process. Furthermore, washing with deionized water neutralized the sample and removed all impurities.

Leaching process was carried out after the washing stage was completed. Leaching or extraction in this aimed to remove Fe from polymer matrix. Leaching process of Fe^{3+} using HCl solution effectively bound Fe(III) metal ions without dissolving or damaging polymer matrix, which was a crucial part of the template formation process in polymer (Kim et al., 2018). As an extraction solvent, HCl had several advantages over other acid solutions. According to previous studies, low silica dioxide solubility and selective crystallization towards metal ions, and could be reused in leaching process (Valeev et al., 2018). The use of HCl in the extraction process allowed the solvent to dissolve more than 90% of Fe at atmospheric pressure by exploiting the difference in reactivity between Fe and aluminum minerals (Sokolov et al., 2021). Leaching process caused a color change from reddish-orange to a striking pale orange, which was noticeable between before and after the process. This occurred because H^+ ions from HCl were covalently bound with Fe(III) ions, which were factors contributing to the reddish-orange color. The longer or repeated leaching process, the more H+ ions continuously bound with Fe(III) ions. This led to the dissolution and reduction of the ions from polymer matrix, as shown by the fading of the sample color (Novianty et al., 2023). When Fe(III) ions were lifted from polymer matrix, templates or pores with shapes, properties, and characteristics, which were almost identical to the physical and chemical structure of the materials removed were formed (Royani and Abdullah, 2019). With these characteristics, Fe(III)-IIPs materials exhibited excellent selectivity towards Fe(III) metal ions, and upon encountering these active substances again, IIPs immediately recognized and bound the active substances in the template,

© 2024 The Authors.

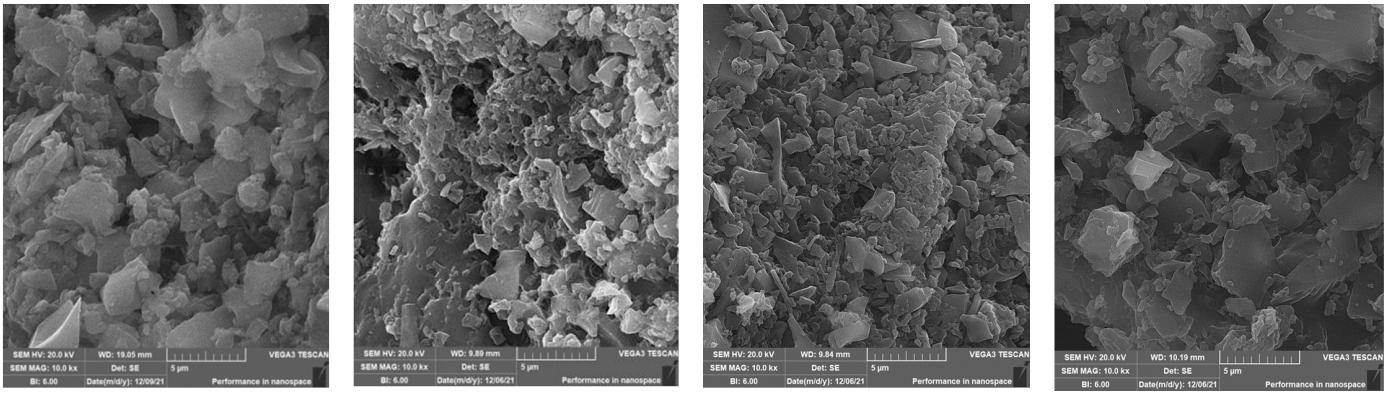

Figure 4. Imaging the Surface Morphology of IIPs Samples with Variations in HCl Solution concentration and temperature (a) 3 M room Temperature, (b) 1 M Room Temperature, (c) 1 M at 60 °C, and (d) 1.5 M HCl at 60 °C

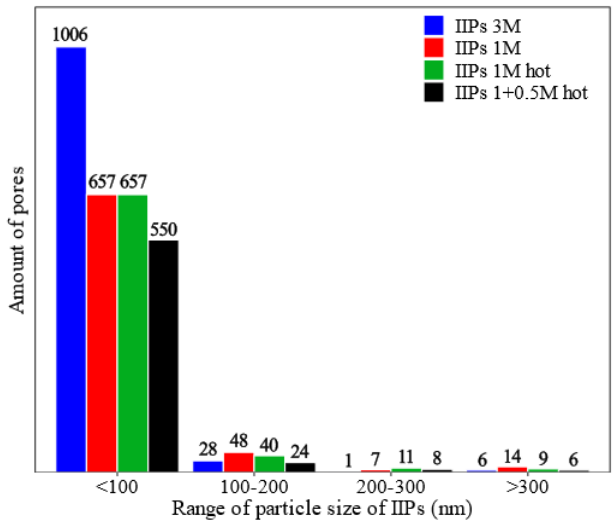

Figure 5. Distribution of Pore Size Distribution of Fe(III) Ion Imprinted Polymers in SEM Imaging with a Magnification of 10,000 Times

commonly referred to as adsorption applications (Roushani et al., 2016).

3.3 Analysis of X-Ray Diffraction (XRD) Results

XRD characterization used to analyze the structure and crystal size of Fe(III)-IIPs could be calculated using the Debye Scherer equation as presented in Equation (5).

$$D = \frac{k.\lambda}{B\cos\theta} \quad (5)$$

D represents the crystal size of Fe(III)-IIPs on a nanometer scale. The Scherrer constant (k) in the formula above took into account the particle shape and was generally considered to be 0.9 (Royani and Abdullah, 2019), λ is wavelength, and B or FWHM is the full width at half maximum (Ullah et al., 2020). The crystal size distribution of unleached Fe(III)-IIPs or Fe(III) polymer with polymer material that had undergone washing with several parameters is presented in Table 2. The synthesized Fe(III)-IIPs had a crystal size distribution on a nanometer scale, indicating an increasingly extensive sample surface. The distribution of nanometer-scale crystal sizes could expand the sample surface contact, making the particles more reactive with the solvent to enhance IIPs template formation process. Extraction experiments with variations in temperature increase indicated limited dissolution of Fe(III) analyte due to the lower solubility of Fe in HCl (Jansen et al., 2011). The extraction process using HCl required a significant amount of energy to interact directly with Fe(III) analyte in polymer matrix, necessitating repetition. The solubilization of Fe in the extraction process led to the formation of cavities in polymer matrix known as templates without disrupting its crystal structure, as shown in Figure 2. The results showed that there was a matching of peak intensities and angle values between IIPs samples with 1 M and 3 M variations and the heat-treated sample.

IIPs samples without an extraction process (unleached) had Fe(III) crystal structure that was similar to a monoclinic crystal structure, where the presence of the active substance Fe(III) in polymer body was still confirmed. Due to the extraction process, the half-maximum peak width value decreased as the crystal size of the sample increased apart from IIPs 3 M. The FWHM value of IIPs 3 M was the widest compared to other samples. A crystal grain size of less than 120 nm caused a widening of XRD spectrum peak.

3.4 Analysis of FTIR Results

Figure 3 shows the characterization results of IIPs samples using FTIR. Furthermore, there was wavelength agreement among Fe polymer samples that had not been washed, including IIPs 3 M, 1 M, 1 M hot, and 1.5 M hot. This indicated that the washing process did not alter the chemical compound

© 2024 The Authors.

Table 3. Comparison of Iron Adsorption with Similar Studies

Monomer	Inhibition Treatment	Equilibirum Time (min)	Adsorption Capacity ($mg.g^{-1}$)	Percent Removal	References
methyl methacrylate	Atmospheric nitrogen	60	122.30	No data	(Darmawan et al., 2020)
4-vinylpyridine	Dry nitrogen	20	1.60	98%	(Mitreva et al., 2017)
methacrylic acid	Atmospheric nitrogen	15	40.41	95%	(Roushani et al., 2016)
methacrylic acid	-5 °C refrigerator-storage ~1h	40	9.35	93%	This study

Table 4. PFO and PSO Equation Parameters in Fe(III) Adsorption

Adsorption Kinetic Equation	Parameter	Results
PFO-Nonlinear Model	q_e ($mg.g^{-1}$)	9.348
	AIC	11.489
	BIC	10.261
	SE	0.873
	RSE	10.744%
PFO-Linear Model	k_1 (min^{-1})	0.0707
	R^2	98.78%
PSO-Nonlinear Model	q_e ($mg.g^{-1}$)	9.348
	AIC	15.625
	BIC	14.398
	SE	1.463
	RSE	18.019%
PSO-Linear Model	k_2 ($g.mg^{-1}.min^{-1}$)	0.024
	R^2	57.657%

arrangement and the functional groups of the materials. The results revealed that the extraction process influenced the percent transmittance produced for each functional group in the samples. In the wavenumber range of 1485-1445 cm^{-1}, the presence of the C−H functional group, which was the methylene group, was confirmed. This functional group indicated the presence of methacrylate acid composition as a successfully synthesized functional monomer in polymer matrix. In addition, the crosslinker compound EGDMA could be analyzed through C−O functional group at wavenumbers between 1300-1000 cm^{-1}. BPO compound as an initiator could be identified through the presence of C=O functional group located at wavenumbers between 1750-1705 cm^{-1}. Both C−O and C=O functional groups were part of the carboxylic acid group. In the unleached Fe(III) polymer sample, the presence of Fe(III) metal ions was confirmed. This could be analyzed through functional groups located at wave numbers 680-610 cm^{-1} or 1386-1350 cm^{-1}, which was part of the group of common inorganic compounds (Huang et al., 2010). IIPs samples that had undergone a washing process using HCl solution also contained functional group, indicating the presence of Fe(III) ions in IIPs samples. This provided information that the extraction process did not remove Fe(III) metal ions completely. In NIP polymer, there was no indication of the presence of Fe(III) ions, as shown in Figure 3.

3.5 Analysis of SEM Results

SEM-EDS characterization was carried out to assess the surface morphology of Fe(III) polymer samples after washing and extraction processes using HCl solution with and without temperature variations. Figure 4 shows the surface structure of IIPs with a widely dispersed size distribution at a magnification of 10,000 times. The successfully synthesized IIPs had cavities on the surfaces that accumulated in different amounts for each extraction variation. The analysis of the number of cavities/pores formed in IIPs could be performed using digital calculation methods, such as Matlab software for analysis using Poredize. Poredize method comprised segmentation and estimation of the physical properties of the material. The segmentation process divided SEM imaging colors with pores as binary number 1, and binary number 0 for polymer matrix that was not a pore.

Due to the extraction process, IIPs materials had the most widespread pore size distribution on the nanometer scale (<100 nm) (Figure 5). The 3 M IIPs had the highest total number of pores, namely 1041, with 96.64% being accumulated on the nanometer scale. The increasing number of pores indicated a larger surface area, making each particle more reactive towards an analyte to fill the template in polymer matrix. This was crucial in adsorption applications that could enhance the recognition sites for better targeting of ion. The surface of IIPs sample with an increasing number of pores significantly influenced the improvement of adsorption capacity of the material (Zhu et al., 2020).

3.6 Fe(III)-IIPs Adsorption Experimental Analysis

Adsorption capacity of the material was analyzed using Atomic absorption spectroscopy (AAS) through Equation (1) and Equation (2) to calculate the efficiency of Fe(III) metal ion adsorption in the solutions. The adsorption process occurs through physical or physisorption, where Van der Waals forces lead to the electrostatic attraction between molecules and fluid interactions on the surface of Fe(III)-IIPs pores (Belmabkhout et al., 2016; Xia et al., 2019). Each analyte ion in the solution filled the reactive surface pores of IIPs, which had physical properties and characteristics similar to the target ion. This was because the reactive surface pores of Fe(III)-IIPs, due to the distribution of crystal sizes on the nanometer scale, made the material more selective towards ion movement.

Table 3 shows a comparison of iron adsorption among several similar studies. The equilibrium time has been reached at 40 minutes adsorption, with a total of 93% Fe(III) ions being

© 2024 The Authors.

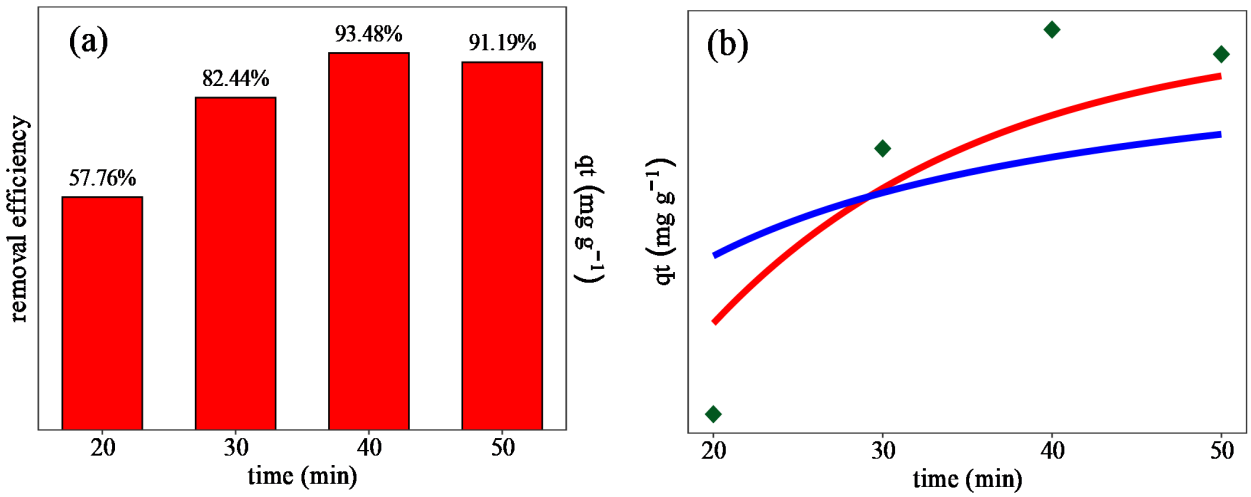

Figure 6. (a) Fe(III) Ion Adsorption Efficiency and (b) Fe(III)-IIPs Adsorption Capacity Modeling

adsorbed. Eventually, we still suffered from relatively low adsorption capacity compared to others, with the maximum at 9.35 $mg.g^{-1}$. The preferable visual representation was shown in Figure 6, where (a) a bar chart of adsorption capacity and efficiency was presented and (b) adsorption modeling to the PFO and PFO equation. However, it still needs further studies to maximize the potential of Fe(III)-IIPs as selectively adsorbent for Fe(III), with optimization in the pH of the adsorbate solution (Palapa et al., 2023).

The assessment parameters used, namely AIC, BIC, and SE, had smaller values in the PFO model compared to the PSO model, indicating a good fit of the model to the data (Mohammed et al., 2015; Spiess and Neumeyer, 2010). Therefore, the adsorption process of Fe^{3+} ions by Fe(III)-IIPs followed the PFO equation. To strengthen this information, modeling was also performed on the linear equations of PFO and PSO, showing higher R^2 values for the PFO-linear model. Table 4 shows the calculation results of the applied parameters.

Adsorption kinetics explained the transfer of adsorbate during adsorption process and the factors influencing adsorption rate over time (Ahmad et al., 2022). Adsorption of Fe^{3+} ions on the surface of Fe(III)-IIPs occured through physisorption, as it followed PFO model, which reinforced the statement discussed above (Sha'arani et al., 2019).

4. CONCLUSIONS

In conclusion, variations in HCl concentration and heat treatment in leaching process of Fe(III) were conducted in the synthesis of IIPs based adsorbent material. XRD characterization results showed that variations in the concentration of the solvent and heat treatment in the process did not alter the crystal structure of Fe(III) but impacted the distribution of crystal size in IIPs, approaching the nanometer order. FTIR data indicated that IIPs compound remained stable after the extraction process. In addition, this process did not change the compound or its functional groups but increased the transmittance percentage value of the sample, providing information that the removal process of Fe(III) metal ions was improving. The number of pores in the samples produced after extraction was analyzed using Matlab software using Poredize. The results revealed that each sample had a greater accumulation at the nanometer size. The number of pores in the order of <100 nm was dominated by IIPs with the largest extraction solvent (3 M), totaling 1006 pores. Meanwhile, the results of adsorption experiment showed that IIPs 3 M material had adsorption capacity of 9.35 $mg.g^{-1}$ and a Fe^{3+} ions absorption efficiency of 93.5% with an optimum time of 40 minutes. Adsorption process followed PFO equation, where the process occurred through physisorption. Based on the results, it could concluded that IIPs materials had significant potential in the monitoring, control, and removal of hazardous heavy metal ions in the environment.

5. ACKNOWLEDGMENT

The research/publication of this article was funded by the 2023 Sriwijaya University Public Service Agency DIPA as an additional output. Number SP DIPA-023.17.2.67751512023, On November 30, 2022. In accordance with the Rector's Decree Number: 0188/UN9.3.1/SK/2023, On April 18, 2023.

REFERENCES

Abbas, A., A. M. Al-Amer, T. Laoui, M. J. Al-Marri, M. S. Nasser, M. Khraisheh, and M. A. Atieh (2016). Heavy Metal Removal from Aqueous Solution by Advanced Carbon Nanotubes: Critical Review of Adsorption Applications. *Separation and Purification Technology*, **157**; 141–161

Adibmehr, Z. and H. Faghihian (2019). Preparation of Highly Selective Magnetic Cobalt Ion-Imprinted Polymer Based on Functionalized SBA-15 for Removal CO_2^+ from Aque-

© 2024 The Authors.

ous Solutions. *Journal of Environmental Health Science and Engineering*, **17**(2); 1213–1225

Ahmad, N., F. S. Arsyad, I. Royani, and A. Lesbani (2022). Adsorption of Methylene Blue on Magnetite Humic Acid: Kinetic, Isotherm, Thermodynamic, and Regeneration Studies. *Results in Chemistry*, **4**; 100629

Ahmadi, E., H. Hajifatheali, Z. Valipoor, and M. Marefat (2021). Synthesis, Characterization and Analytical Applications of Ni (II) Ion-Imprinted Polymer Prepared by N-(2-Hydroxyphenyl) Acrylamide. *Journal of Polymer Research*, **28**(181); 1–11

Belmabkhout, Y., V. Guillerm, and M. Eddaoudi (2016). Low Concentration CO_2 Capture Using Physical Adsorbents: Are Metal-Organic Frameworks Becoming the New Benchmark Materials? *Chemical Engineering Journal*, **296**; 386–397

Bezzina, J. P., T. Robshaw, R. Dawson, and M. D. Ogden (2020). Single Metal Isotherm Study of the Ion Exchange Removal of Cu (II), Fe (II), Pb (II) and Zn (II) from Synthetic Acetic Acid Leachate. *Chemical Engineering Journal*, **394**; 124862

Cao, H., P. Yang, T. Ye, M. Yuan, J. Yu, X. Wu, F. Yin, Y. Li, and F. Xu (2021). Recognizing Adsorption of Cd (II) by a Novel Core-Shell Mesoporous Ion-Imprinted Polymer: Characterization, Binding Mechanism and Practical Application. *Chemosphere*, **278**; 130369

Chi, Z., Y. Zhu, W. Liu, H. Huang, and H. Li (2021). Selective Removal of As (III) Using Magnetic Graphene Oxide Ion-Imprinted Polymer in Porous Media: Potential Effect of External Magnetic Field. *Journal of Environmental Chemical Engineering*, **9**(4); 105671

Darmawan, W., D. Nurani, D. Rahayu, and I. Abdullah (2020). Synthesis of Ion Imprinted Polymer for Separation and Preconcentration of Iron (III). In *AIP Conference Proceedings*, volume 2242. AIP Publishing, page 040025

Diale, P., D. Hildebrandt, D. Glasser, T. Matambo, and S. Makgato (2023). An Analysis of the Processes, Kinetics and Equilibrium of Iron's Biosorption on Immobilized Green Microalgae. *South African Journal of Chemical Engineering*, **45**; 210–220

Edianta, J., O. Satya, F. Virgo, K. Saleh, and I. Royani (2023a). Design of Potentiometric Instrumentation System Based on Arduino Nano Microcontroller Using Imprinted Polymer for the Determination of Fe (III) Metal Ions. In *AIP Conference Proceedings*, volume 2689. AIP Publishing, page 2689

Edianta, J., O. C. Satya, K. Saleh, F. Virgo, F. Monado, and I. Royani (2023b). Review of Ion Imprinted Polymers Nanofiber with Technology Electrospinning: An Advanced Materials for Removal of Heavy Metal Ions. *Journal of Chemical Technology & Metallurgy*, **58**(4); 731–738

Huang, H., Y. Ji, Z. Qiao, C. Zhao, J. He, and H. Zhang (2010). Preparation, Characterization, and Application of Magnetic Fe-SBA-15 Mesoporous Silica Molecular Sieves. *Journal of Analytical Methods in Chemistry*, **2010**; 1–7

Huang, L., C. T. Parsons, S. Slowinski, and P. Van Cappellen (2024). Co-Precipitation of Iron and Silicon: Reaction Kinetics, Elemental Ratios and the Influence of Phosphorus. *Chemosphere*, **349**; 140930

Izadi, A., A. Mohebbi, M. Amiri, and N. Izadi (2017). Removal of Iron Ions from Industrial Copper Raffinate and Electrowinning Electrolyte Solutions by Chemical Precipitation and Ion Exchange. *Minerals Engineering*, **113**; 23–35

Jansen, B., F. Tonneijck, and J. Verstraten (2011). Selective Extraction Methods for Aluminium, Iron and Organic Carbon from Montane Volcanic Ash Soils. *Pedosphere*, **21**(5); 549–565

Kasim, N., A. W. Mohammad, and S. R. S. Abdullah (2016). Performance of Membrane Filtration in the Removal of Iron and Manganese from Malaysia's Groundwater. *Membr. Water Treat*, **7**(4); 277–296

Kim, B.-K., E. J. Lee, Y. Kang, and J.-J. Lee (2018). Application of Ionic Liquids for Metal Dissolution and Extraction. *Journal of Industrial and Engineering Chemistry*, **61**; 388–397

Kong, Z., Y. Du, J. Wei, H. Zhang, and L. Fan (2021). Synthesis of a New Ion-Imprinted Polymer for Selective Cr (VI) Adsorption from Aqueous Solutions Effectively and Rapidly. *Journal of Colloid and Interface Science*, **588**; 749–760

Koriyanti, E., K. Saleh, F. Monado, F. Syawali, and I. Royani (2020). On the Effect of Ethanol Solution on Melamine Template Removal Process. *Journal of Chemical Technology and Metallurgy*, **55**(1); 2020

Mahmoud, M. A. (2015). Kinetics and Thermodynamics of Aluminum Oxide Nanopowder As Adsorbent for Fe (III) from Aqueous Solution. *Beni-Suef University Journal of Basic and Applied Sciences*, **4**(2); 142–149

Mhatre, A., C. Agarwal, T. N. Nag, A. Bhattacharyya, and R. Tripathi (2021). Phosphate-Based Ce (IV) Ion-Imprinted Polymers for Separation of Berkelium: Testing the Homologue Imprinting Approach for Heavy Actinides. *ACS Applied Polymer Materials*, **3**(3); 1465–1478

Mitreva, M., I. Dakova, and I. Karadjova (2017). Iron (II) Ion Imprinted Polymer for Fe (II)/Fe (III) Speciation in Wine. *Microchemical Journal*, **132**; 238–244

Mohammed, E. A., C. Naugler, and B. H. Far (2015). Emerging Business Intelligence Framework for a Clinical Laboratory through Big Data Analytics. *Emerging trends in computational biology, bioinformatics, and systems biology: algorithms and software tools. New York: Elsevier/Morgan Kaufmann*; 577–602

Novianty, J. Edianta, Jorena, K. Saleh, A. A. Bama, E. Koriyanti, M. Ariani, and I. Royani (2023). Synthesis of Fe(III)-IIPs (Ion Imprinted Polymers): Comparing Different Concentrations of HCl and HNO_3 Solutions in the Fe(III) Polymer Extraction Process for Obtaining the Largest Cavities in Fe(III)-IIPs. *Science and Technology Indonesia*, **8**(3); 361–366

Palapa, N. R., N. Ahmad, A. Wijaya, and Z. A. Zahara (2023). Facile Fabrication of Layered Double Hydroxide-Lignin for Efficient Adsorption of Malachite Green. *Science and Technology Indonesia*, **8**(2); 305–311

Rais, S., A. Islam, I. Ahmad, S. Kumar, A. Chauhan, and H. Javed (2021). Preparation of a New Magnetic Ion-Imprinted Polymer and Optimization Using Box-Behnken

© 2024 The Authors.

Design for Selective Removal and Determination of Cu (II) in Food and Wastewater Samples. *Food Chemistry*, **334**; 127563

Reis, P. M., J. R. Rodrigues, L. M. Gando-Ferreira, and R. M. Quinta-Ferreira (2024). Optimization of Fenton Process Conditions in Winery Wastewaters Treatment Followed by Ion Exchange Process to Recover Iron. *Journal of Industrial and Engineering Chemistry*, **129**; 365–372

Ricart, D., A. D. Dorado, C. Lao-Luque, and M. Baeza (2024). Microflow Injection Analysis Based on Modular 3D Platforms and Colorimetric Detection for Fe (III) Monitoring in a Wide Concentration Range. *Microchimica Acta*, **191**(1); 3

Rivaro, P., D. Vivado, C. Ianni, A. Salis, A. Parodi, and E. Millo (2024). A New Approach to Characterize Siderophore-Type Ligands in Seawater by Solid Phase Synthesis and SPE-HPLC-ESI-MS/MS Analysis. *Journal of Marine Science and Engineering*, **12**(1); 110

Roushani, M., T. M. Beygi, and Z. Saedi (2016). Synthesis and Application of Ion-Imprinted Polymer for Extraction and Pre-Concentration of Iron Ions in Environmental Water and Food Samples. *Spectrochimica Acta Part A: Molecular and Biomolecular Spectroscopy*, **153**; 637–644

Royani, I. and M. Abdullah (2019). The Effect of Atrazine Concentration on Galvanic Cell Potential Based on Molecularly Imprinted Polymers (MIPS) and Aluminium As Contact Electrode. In *Journal of Physics: Conference Series*, volume 1282. IOP Publishing, page 012029

Royani, I., A. Amalia, J. Jorena, F. S. Arsyad, E. Koriyanti, and F. Monado (2021). The Characteristic Analysis of Caffeine Molecularly Imprinted Polymers Synthesized Using The Cooling-Heating Method, for Application as a Sensor Material. *Science and Technology Indonesia*, **6**(4); 256–260

Royani, I., W. Widayani, A. Mikrajuddin, and K. Khairurrijal (2014). Effect of Heating Time on Atrazine-Based MIP Materials Synthesized via the Cooling-Heating Method. *Advanced Materials Research*, **896**; 89–94

Sala, A., H. Brisset, A. Margaillan, J.-U. Mullot, and C. Branger (2022). Electrochemical Sensors Modified with Ion-Imprinted Polymers for Metal Ion Detection. *TrAC Trends in Analytical Chemistry*, **148**; 116536

Sha'arani, S. A. W., M. A. M. R. S. Khudri, A. R. Othman, M. I. E. Halmi, N. A. Yasid, and M. Y. Shukor (2019). Kinetic Analysis of the Adsorption of the Brominated Flame Retardant 4-Bromodiphenyl Ether onto Biochar-Immobilized *Sphingomonas* Sp. *Bioremediation Science and Technology Research*, **7**(1); 8–12

Sokolov, A., D. Valeev, and A. Kasikov (2021). Solvent Extraction of Iron (III) from Al Chloride Solution of Bauxite HCl Leaching by Mixture of Aliphatic Alcohol and Ketone. *Metals*, **11**(2); 321

Spiess, A.-N. and N. Neumeyer (2010). An Evaluation of R^2 As an Inadequate Measure for Nonlinear Models in Pharmacological and Biochemical Research: A Monte Carlo Approach. *BMC Pharmacology*, **10**(1); 1–11

Taheri, Z., A. Afkhami, T. Madrakian, and M. Kamalabadi (2021). Application of Magnetic Ion Imprinted Polymers for Simultaneous Quantification of $Al^{3+}$and Be^{2+} Ions Using the Mean Centering of Ratio Spectra Method. *Talanta*, **225**; 122003

Ullah, S., M. Hashmi, N. Hussain, A. Ullah, M. N. Sarwar, Y. Saito, S. H. Kim, and I. S. Kim (2020). Stabilized Nanofibers of Polyvinyl Alcohol (PVA) Crosslinked by Unique Method for Efficient Removal of Heavy Metal Ions. *Journal of Water Process Engineering*, **33**; 101111

Valeev, D., A. Mikhailova, and A. Atmadzhidi (2018). Kinetics of Iron Extraction from Coal Fly Ash by Hydrochloric Acid Leaching. *Metals*, **8**(7); 533

Wang, L., B. Li, J. Wang, J. Qi, J. Li, J. Ma, and L. Chen (2022). A Rotary Multi-Positioned Cloth/paper Hybrid Microfluidic Device for Simultaneous Fluorescence Sensing of Mercury and Lead Ions by Using Ion Imprinted Technologies. *Journal of Hazardous Materials*, **428**; 128165

Wyns, K., N. Gys, A. D. Varela, J. Spooren, T. A. Atia, E. M. Seftel, and B. Michielsen (2021). Iron (III) Removal from Acidic Solutions Using Mesoporous Titania Microspheres Prepared by Vibrational Droplet Coagulation. *Journal of Environmental Chemical Engineering*, **9**(5); 106257

Xia, M., Z. Chen, Y. Li, C. Li, N. M. Ahmad, W. A. Cheema, and S. Zhu (2019). Removal of Hg (II) in Aqueous Solutions through Physical and Chemical Adsorption Principles. *RSC Advances*, **9**(36); 20941–20953

Zhang, X., X. Ou, J. Zhang, Z. Chen, C. Liu, H. Li, X. Li, Y. Sun, Z. Chen, and J. Zhu (2021). Smart Ion Imprinted Polymer for Selective Adsorption of Ru (III) and Simultaneously Waste Sample Being Transformed As a Catalyst. *Journal of Hazardous Materials*, **417**; 126072

Zhao, Z., H. Jiang, L. Wu, N. Yu, Z. Luo, and W. Geng (2022). Preparation of Magnetic Surface Ion-Imprinted Polymer Based on Functionalized Fe_3O_4 for Fast and Selective Adsorption of Cobalt Ions from Water. *Water*, **14**(2); 261

Zhu, G. J., H. Y. Tang, P. H. Qing, H. L. Zhang, X. C. Cheng, Z. H. Cai, H. B. Xu, and Y. Zhang (2020). A Monophosphonic Group-Functionalized Ion-Imprinted Polymer for a Removal of Fe^{3+} from Highly Concentrated Basic Chromium Sulfate Solution. *Korean Journal of Chemical Engineering*, **37**(5); 911–920

© 2024 The Authors.